# Numerical investigation of high-speed droplet impact using a multiscale two-fluid approach

Georgia Nykteri *[1], Phoevos Koukouvinis[1], Silvestre Roberto Gonzalez Avila[2], Claus-Dieter Ohl[2], Manolis Gavaises[1]
[1]School of Mathematics, Computer Science & Engineering, Department of Mechanical Engineering & Aeronautics, CITY University of London, Northampton Square EC1V 0HB, United Kingdom
[2]Institute of Physics, Otto-von-Guericke University Magdeburg, Universitätsplatz 2, 39016 Magdeburg, Germany
*Corresponding author: georgia.nykteri@city.ac.uk

**Abstract**
A single droplet impact onto solid surfaces remains a fundamental and challenging topic in both experimental and numerical studies with significant importance in a plethora of industrial applications, ranging from printing technologies to fuel injection in internal combustion engines. Under high-speed impact conditions, additional complexities arise as a result of the prompt droplet splashing and the subsequent violent fragmentation; thus, different flow regimes and a vast spectrum of sizes for the produced secondary flow structures coexist in the flow field. The present work introduces a numerical methodology to capture the multiscale processes involved with respect to local topological characteristics. The proposed methodology concerns a compressible Σ-Y two-fluid model with dynamic interface sharpening based on an advanced flow topology detection algorithm. The model has been developed in OpenFOAM® and provides the flexibility of dealing with the multiscale character of droplet splashing, by switching between a sharp and a diffuse interface within the Eulerian-Eulerian framework in segregated and dispersed flow regions, respectively. An additional transport equation for the interface surface area density (Σ) introduces important information for the sub-grid scale phenomena, which is exploited in the dispersed flow regions to provide an insight into the extended cloud of secondary droplets after impact on the target. A high-speed water droplet impact case has been examined and evaluated against new experimental data; these refer to a millimetre size droplet impacting a solid dry smooth surface at velocity as high as 150m/s, which corresponds to a Weber number of ~$7.6\times10^5$. At the investigated impact conditions compressibility effects dominate the early stages of droplet splashing. A strong shock wave forms and propagates inside the droplet, where transonic Mach numbers occur; local Mach numbers up to 2.5 are observed for the expelled surrounding gas outside the droplet. The proposed numerical approach is found to capture relatively accurately the phenomena and provide significant information regarding the produced flow structure dimensions, which is not available from the experiment.

**Keywords**
two-fluid model; compressible Navier-Stokes; Σ-Y formulation; adaptive flow topology detection; droplet impact

## Introduction

Multiscale complexities are realised in numerous multiphase flow fields of both industrial and more theoretical interest due to the temporal and spatial geometric diversity of the flow patterns formed by the interacting phases. Examples from the plethora of multidisciplinary applications include fuel spray injection in internal combustion engines, droplet aerodynamic-induced breakup occurring in all type of liquid-fuel combustors, droplet splashing, and even the Rayleigh–Taylor instability in a supernova explosion. Several numerical approaches have been proposed in the literature over the years, regarding the modelling of multiphase flows in engineering applications. Among the most classic models are the Discrete Droplet Method (DDM) [1], the homogeneous mixture model [2] and the inhomogeneous mixture model [3], often referred to as the multifluid model. Recently, more advanced numerical models have been developed in order to overcome the dependency on local flow regimes in specific multiphase flow applications. The ELSA model [4] provides a dynamic transition between an Eulerian and a Lagrangian framework in the primary and secondary liquid spray atomization regions, respectively. The additional transport equation for the liquid gas interface surface area density (Σ) allows for the representation of unresolvable sub-grid scale structures with a viable computational cost, ought to the physical modelling of the mechanisms responsible for the interface surface area formation [5]. A further insight into the sub-grid scale phenomena can be gained with the implementation of a probability density function (PDF) so as to obtain secondary droplet size distributions and other stochastic properties of the dilute spray using the Method of Moments [6] or the joint sub-grid scale volume surface PDF [7]. With respect to commercial CFD codes, a complete atomization model for liquid fuel spray simulations has been integrated in AVL FIRE®, using a fully Eulerian formulation [8]. In the recent versions

of OpenFOAM® a hybrid fully Eulerian incompressible solver has been implemented, namely multiphaseEulerFoam [9], which supports a dynamic switching between a diffuse and a sharp interface approach within the same multifluid framework. However, the advantages of the state-of-the-art numerical models over the more classic approaches are restricted to the needs of the specific applications for which they were developed.

The above methodologies can be applied to the case of a droplet impacting on solid surfaces, which represents a fundamental multiscale flow problem, that still attracts the scientific interest. The droplet deformation and potential fragmentation after impact is very sensitive to several parameters regarding the impact and target conditions and the post-impact outcomes are subject to different regimes, ranging from spreading or even sticking on the surface to rebounding and splashing. Even though the single droplet impact onto solid surfaces has been extensively investigated with experimental studies since 1877, the mechanisms of the prompt and violent splashing under high impact velocities, which correspond to the massive spatial dispersion of the produced secondary droplets far away from the solid surface and the dominance of compressibility phenomena with strong propagating shock waves inside the deforming droplet, have not been precisely revealed yet. Recent experimental studies in the literature mainly focus on the early stages of the droplet and wall interaction and do not exceed impact Weber number values of 2500 (see selectively [10], [11]). Regarding the numerical investigation of droplet impact cases, most recent studies examine the impact on solid surfaces, utilizing an interface capturing method for the conducted simulations (see selectively [12], [13]). With the VOF method to be the most commonly used approach, the droplet deformation and spreading on the target can be captured in detail with a sufficiently fine mesh. However, in the case of higher impact velocities, which result to splashing and fragmentation of the droplet into secondary microscale structures, the performed simulations are restricted to the early stages of the phenomena, since the later stages of droplet fragmentation are dominated by computationally prohibitive scales for a VOF simulation. Thus, a more advanced numerical modelling is required to deal simultaneously with the early and later stages of the splashing droplet evolution. Moreover, other studies perform high-speed droplet impact simulations with the focus on capturing the occurring compressibility phenomena that dominate during the early stages of the impact (see selectively [14], [15], [16], [17]).

Following the limitations of the currently used numerical methodologies in multiscale flow applications, the present study proposes a multiscale numerical framework [18] which has been developed in OpenFOAM® utilizing the two-fluid formulation [3]; this allows for both compressibility and slip velocity effects to be taken into account. The model solves for an additional transport equation for the interface surface area density (Σ) [4] to provide an insight into the unresolved sub-grid scale phenomena which are related to the interface formation. The Σ-Y two-fluid model is also combined with a dynamic switching between the sharp and the diffuse interface approaches, applicable in segregated and dispersed flow regions, respectively. A key factor for the accurate functioning of the multiscale formulation is the advanced flow topology detection algorithm, which can detect instantaneous topological changes in flow regimes and allow for a flexible two-way switching between the two different interface approaches. Validation of the proposed numerical model is performed against a high-speed water droplet impact case, using new experimental data. Finally, emphasis from the numerical perspective is given on capturing the dispersed regions of the flow field at the later stages of the droplet fragmentation evolution, where even the experimental investigation cannot contribute with sufficient information due to limitations in diagnostic methods for high Mach number flows consisting of a large number of droplets with sizes less than 1μm.

**Numerical Method**

The Σ-Y two-fluid model with dynamic local topology detection [18] has been implemented in OpenFOAM® with further developments on twoPhaseEulerFoam solver, an available compressible fully Eulerian implicit pressure-based solver. In principle, the numerical model consists of the same set of governing equations for both multiscale formulations, namely the sharp and the diffuse interface approach, with specific source terms to be activated and deactivated depending on the currently operating formulation of the solver, as it is described in detail below.

*Two-Fluid Model Governing Equations*

In the context of a two-fluid approach [3], the volume averaged conservation equations governing the balance of mass, momentum and energy are solved separately for each phase k:

$$\frac{\partial}{\partial t}(a_k\rho_k) + \nabla\cdot(a_k\rho_k u_k) = 0 \quad (1)$$

$$\frac{\partial}{\partial t}(a_k\rho_k u_k) + \nabla\cdot(a_k\rho_k u_k u_k) = -a_k\nabla p + \nabla\cdot\left(a_k\boldsymbol{\tau}_k^{eff}\right) + a_k\rho_k g + \sum_{\substack{n=1\\ n\neq k}}^{2} M_{kn} \quad (2)$$

$$\frac{\partial}{\partial t}[a_k\rho_k(e_k+k_k)] + \nabla\cdot[a_k\rho_k(e_k+k_k)u_k] = -\nabla\cdot\left(a_k\boldsymbol{q}_k^{eff}\right) - \left[\frac{\partial a_k}{\partial t}p + \nabla\cdot(a_k u_k p)\right] + a_k\rho_k g\cdot u_k + \sum_{\substack{n=1\\ n\neq k}}^{2} E_{kn} \quad (3)$$

$M_{kn}$ represents the forces acting on the dispersed phase and depends on local topology; the surface tension force [19] is implemented under the sharp interface regime, while the aerodynamic drag force [20] is implemented under

the diffuse interface regime. On the contrary, $E_{kn}$ demonstrates the heat transfer between the phases that can be modelled via a standard heat transfer law, irrespectively of the flow region. Phase-change phenomena are neglected since they are negligible in the examined high-speed droplet impact case [15], [16]. LES is used for the turbulence modelling with the implementation of the one-equation SGS model [21]; the two-layer wall function is implemented. Finally, for thermodynamic closure of the system the ideal gas equation of state is utilized for the gaseous phase and the stiffened gas equation of state [22] has been implemented and utilized for the liquid phase.

*Σ-Y Model Transport Equations*

The transport equation for the liquid volume fraction in a compressible two-phase flow is:

$$\frac{\partial a_l}{\partial t} + \nabla \cdot (a_l u_m) + v_{topo}[\nabla \cdot (a_l(1-a_l)u_c)] = a_l a_g \left(\frac{\psi_g}{\rho_g} - \frac{\psi_l}{\rho_l}\right)\frac{Dp}{Dt} + a_l \nabla \cdot u_m - \left(1 - v_{topo}\right)R_{a_l} \quad (4)$$

where $v_{topo}$ allows for distinguishing between the two different interface approaches by taking either 0 or 1 value under a diffuse or sharp interface formulation, respectively. Interface sharpness is imposed with the MULES algorithm in OpenFOAM® [23], which introduces an artificial compression term in equation (4). Additional modifications in the governing equations for coupling the VOF method with the two-fluid framework have been previously presented in detail in [18]. $R_{al}$ [4], [24] accounts for the liquid dispersion induced by turbulent velocity fluctuations, which are important in dispersed flows and smaller scales.

The transport equation for the liquid gas interface surface area density (Σ) [5] is described as follows:

$$\frac{\partial \Sigma'}{\partial t} + \nabla(\Sigma' u_m) = (1 - v_{topo})\left[-R_\Sigma + C_{SGS}\frac{\Sigma}{\tau_{SGS}}\left(1 - \frac{\Sigma}{\Sigma^*_{SGS}}\right)\right] \quad (5)$$

where the simultaneous existence of liquid and gas on the interface implies the presence of a minimum interface surface area density [25], such as: $\Sigma = \Sigma' + \Sigma_{min}$. $R_\Sigma$ [24] represents the interface surface area diffusion due to turbulent velocity fluctuations. The second source term on the RHS of equation (5) accounts for all physical mechanisms which fall below the computational mesh resolution and are responsible for the local interface production and destruction, among which turbulence, droplet collision, coalescence and secondary breakup effects are taken into consideration [5].

*Flow Topology Detection Algorithm*

Assuming that at least 3 computational cells are needed for the grid resolution to capture any spherical structure with sufficient sharpness [26], a geometric criterion for the diameter of an equivalent spherical structure based on the local interface curvature can be proposed as the limit for the sharp interface approach:

$$d_{curv} < 3 * max(d_{cell}) \quad (6)$$

Nevertheless, this geometric criterion can only be considered as an indication for a potential switch to a diffuse interface approach. All computational cells which meet criterion (6) are subject to a second stage of topological examination based on the condition of their neighbour cells. The three different possibilities are as follows:

- A single cell which is supposed to follow a diffuse interface approach based on the geometric criterion but belongs to a strictly segregated region with sharp interfaces, will remain unaffected by changes, as shown in Figure 1(a).
- When a cell is part of a topologically unstable region, where all its neighbour cells previously respected a sharp interface approach but now some of them are also subject to changes, then as depicted in Figure 1(b), an expanded region is examined. Specifically, the surrounding area of the neighbour cells which are of particular interest is evaluated with regards to the occurring topological conditions. Finally, if the examined cell belongs to a highly transitional region, then the topological criterion is met and a change for the interface approach is applied.
- As illustrated in Figure 1(c), any cell that is in the border of transition between segregated and highly dispersed flow regimes will follow the tendency of local interface formation and will be subject to the diffuse interface approach in the following time step.

However, the reset of a sharp interface approach for a previously diffuse cell is performed after meeting a single geometric criterion based on $d_\Sigma$ [25] without examining the surrounding flow conditions, as illustrated in Figure 1(d):

$$d_\Sigma > min(d_{cell}) \quad (7)$$

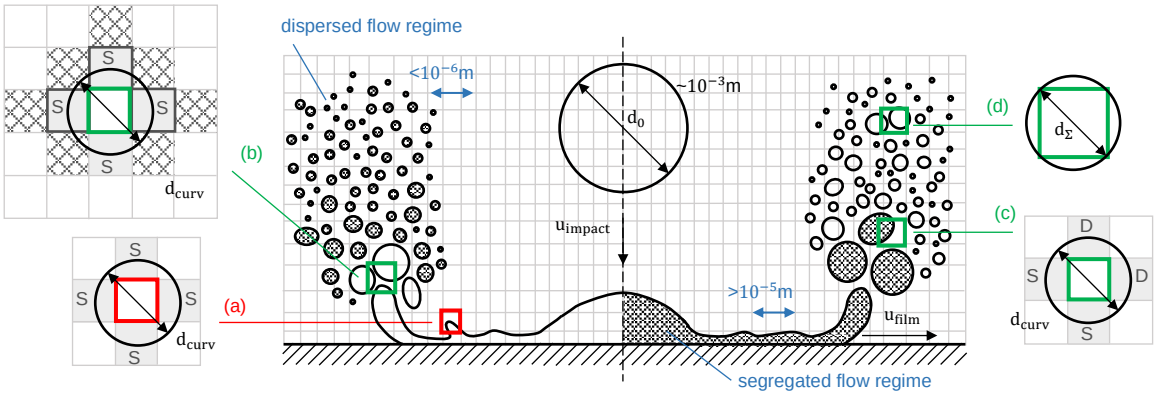


**Figure 1.** Local topology detection and distinction criteria between the segregated and the dispersed flow regimes. Application to the multiscale flow of a millimetre size droplet impact on a rigid wall with indicative dominant scales under each flow regime.

## Results and discussion

*Experimental Set-up*

In order to validate the multiscale approach developed, new experiments have been performed for a droplet impact onto a solid surface. The experiments have been conducted at the University of Magdeburg and concern a water droplet impact onto a high-speed moving target. The deionized water droplet is slightly deformed to an ellipsoid shape, due to the acoustic field which keeps it levitated, with radius 1.325mm and 1.1mm in the horizontal and vertical direction, respectively. The flat and smooth moving target is manufactured from teflon and is propelled with a velocity of 150m/s from an initial distance of 2.35m away from the levitating droplet. The experiment was performed at room temperature 21ºC, atmospheric pressure conditions and surface tension between the water droplet and the surrounding air equal to 0.072N/m. The occurring impact conditions correspond to high Weber and Reynolds numbers with values $7.6\times10^5$ and $3.7\times10^5$, respectively, as calculated for the droplet properties at impact conditions. The prompt droplet splashing was visualized with the use of a high speed camera of 5 million frames per second and a spatial resolution of 50μm per pixel; recording of video started when the moving target was approximately 3.17mm away from the droplet.

*Simulation Results*

For the numerical simulation of high-speed droplet fragmentation, the problem is set-up in a different but corresponding manner with the water droplet moving with an initial velocity of 150m/s towards a rigid wall target. The simulation was performed in a 3D wedge geometry with one cell thickness, using a computational mesh of 412,500 cells; the details are described in Figure 2. At the initial time-step the moving droplet is set 0.9mm away from the rigid wall. Apart from the liquid phase velocity field, which is initialized with the initial velocity of the moving droplet, i.e. 150m/s, the air velocity field is also initialized from a developed field obtained with an inlet velocity of 150m/s from the right patch of the computational domain. Using this configuration, the effect of the moving target on the surrounding air in the original experimental set-up is adequately represented in the conducted simulation. The liquid gas interface density is initialized on the droplet interface as the surface area of an ellipsoid with the dimensions of the water droplet which corresponds to a 5º wedge per unit of the local computational cell volume. On the wall, a no-slip boundary condition is applied for the velocity fields, while a Neumann boundary condition is satisfied for the other computed flow fields. The spatial discretization used is based on second order limited linear discretization schemes. Time stepping is performed adaptively during the simulation, so as to respect the selected limit for the convective Courant–Friedrichs–Lewy (CFL) condition of 0.4. Even though the turbulent state corresponds to fully 3D-developed phenomena, the evolution of the droplet fragmentation is found to be significantly quicker compared to the turbulence time scales. Therefore, the configuration of Figure 2 is an acceptable compromise between the accuracy of the numerical model and a viable computational cost. Since the droplet impact evolution is not driven by cavitation [15], [16], a model for cavitation has not been implemented; instead, a very small volume fraction of air in order of $10^{-6}$, which corresponds to the nucleation volume fraction, is introduced in the initial droplet volume fraction. Under this assumption, the small gaseous volumes inside the droplet will expand after the significant pressure drop, leading to volumes equal to those that would occur with cavitation.

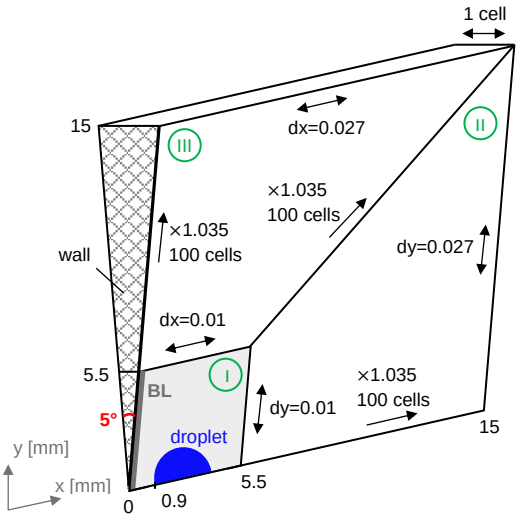


**Figure 2.** Initial configuration and computational mesh used in the simulation of a high-speed droplet impact on a rigid wall.

The evolution of the droplet fragmentation at 2, 4 and 6μs after the impact on the target is presented in Figure 3, as it has been captured by the experimental study and the performed simulations with the proposed multiscale two-fluid approach. In the numerical investigation, the widespread and highly dispersed water cloud produced after the prompt splashing of the droplet is subject to the diffuse interface formulation of the multiscale two-fluid approach, shown as a grey iso-surface in the results. Therefore, the dominant sub-grid scale structures are modelled accordingly within the dispersed flow regime formulation of the numerical model and the interface surface area density diameters are calculated. Despite the vast spectrum of scales involved, the macroscopic characteristics of the successive stages of the droplet fragmentation are adequately predicted by the performed simulations, with the corresponding results to depict the widespread water dispersion in the form of a radially expanding droplets cloud.

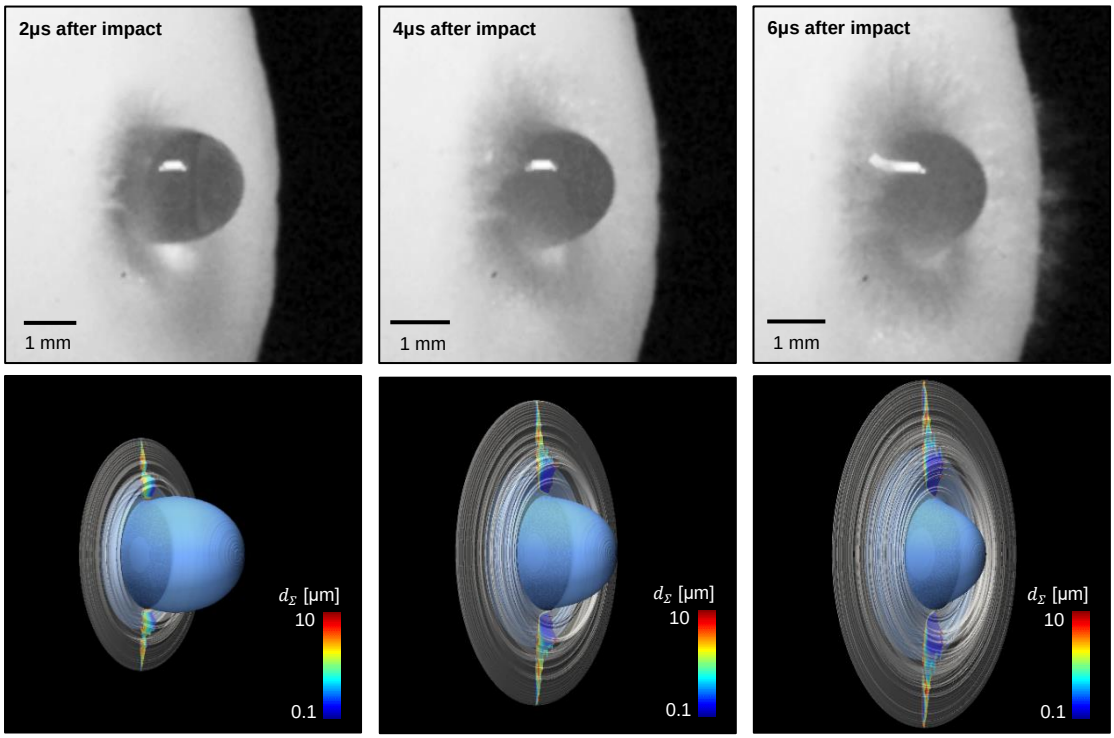


**Figure 3.** Droplet fragmentation at successive time instances. Comparison between the experimental results 32º from the perpendicular view and the 3D reconstructed flow fields from the simulation. Blue iso-surface represents the water volume fraction value of 0.5 and grey iso-surface the diffuse interface regions calculated with the multiscale two-fluid approach.

The droplet impact and the subsequent violent fragmentation under the examined impact conditions evolve rapidly in space and time with different dominant flow regimes at the earlier and the later stages of the phenomenon. In successive time instances in Figure 4, the experimental results are compared with the 3D reconstructed water volume fraction iso-surface at $10^{-3}$ obtained from the performed simulations with the proposed multiscale two-fluid approach and the compressibleInterFoam solver, which is based on a VOF method commonly used for this type of

problems. The violent impact conditions do not allow for a liquid lamella to be formed, as depicted in the experimental results at the early stages of the impact; instead, the production of a dense cloud of secondary droplets is observed. At these stages, which correspond to 22 and 24μs in Figure 4, the topological algorithm detects the first transitions in the dispersed flow regime; the cloud of the produced fluid structures after the droplet and wall impact is subject to a diffuse interface approach, since it consists of structures smaller than $10^{-5}$m that cannot be resolved by the local mesh resolution. On the contrary, the simulation with a VOF method applied in the whole flow field captures accurately the tendency of a radial water expansion. However, the overall sharp interface formulation leads to the prediction of an unphysical thin water film, as in the case of a well-formed lamella under moderate impact conditions, instead of the experimentally observed wide cloud of secondary droplets. At the later stages of the impact, namely at 26 and 28μs in Figure 4, the flow is highly dispersed with an extended cloud of secondary features expanding radially away from the target. A widespread dispersed region in the form of an expanding corona is also captured by the multiscale two-fluid approach, providing an accurate insight into the presence of an extended and chaotic water dispersion. On the contrary, the VOF method results are restricted to a non-realistic water film spreading with only a few droplets being formed as a numerical result of the strict sharp interface implementation.

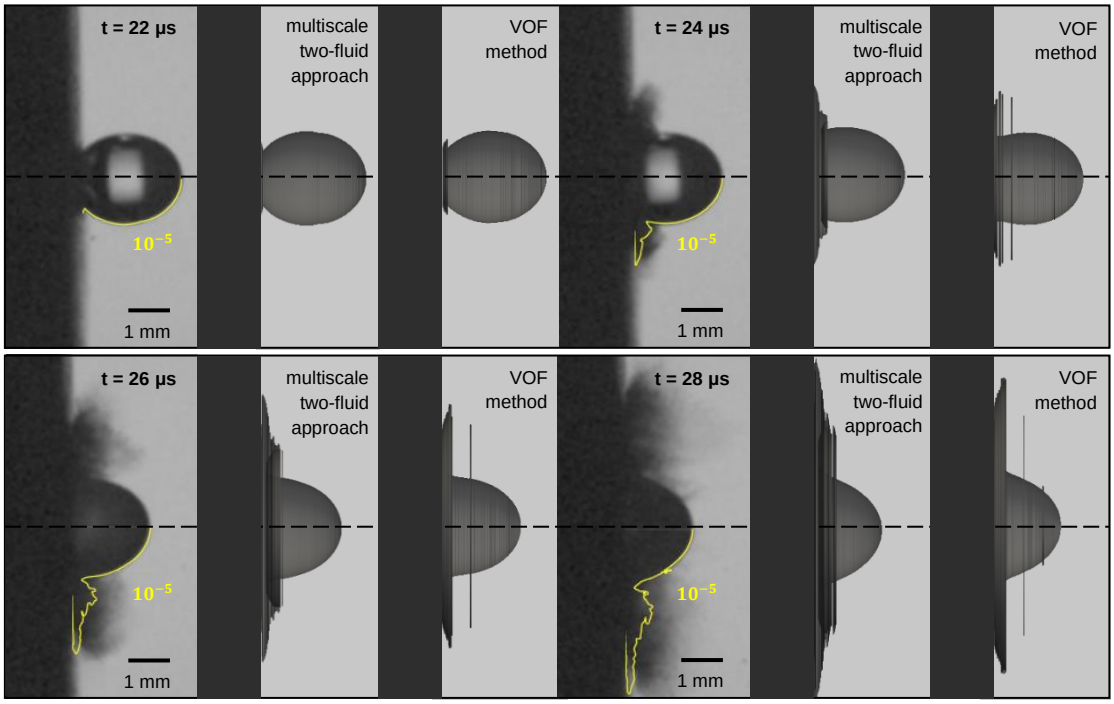


**Figure 4.** Early and later stages of droplet impact on the target. Comparisons between the experimental results from side view and the 3D reconstructed water volume fraction iso-surface at $10^{-3}$ obtained with the multiscale two-fluid approach and the VOF method. Yellow iso-line represents the water volume fraction at $10^{-5}$, calculated with the multiscale two-fluid approach.

The high-speed droplet impact is governed by significant compressibility effects inside the droplet at the early stages of the interaction with the rigid wall. At the moment that the droplet reaches the wall, a strong shock wave is formed inside the droplet with local pressure up to 1200bar, as depicted in Figure 5 at 21.2μs. The shock wave is propagating and moving outwards, opposite to the droplet motion, while it gradually overtakes the contact line between the target and the deforming droplet. At 21.8μs it is observed that the shock wave is reflected normal to the droplet outer free surface and an expansion wave adjacent to the free surface is created [14], [17]. Afterwards, the shock wave propagation continues with the formation of an increasing low pressure region inside the droplet, until the time it reaches the boundary of the deforming droplet interface and it is reflected backwards at 23.9μs. This shock wave reflection results to the creation of strong rarefaction waves at 24μs, which could result to cavitation regions inside the droplet [14], [17]. Along with the shock wave propagation inside the droplet, a supersonic flow with strong propagating shock waves is observed in the surrounding air, due to the high speed dispersion of the produced water cloud. As illustrated in Figure 5, the formation and high-speed injection of the water film at the early stages of the droplet impact, corresponds to a violent displacement of the surrounding air, resulting to a supersonic flow for the air with local Mach numbers up to 2.5. Subsequently, during the droplet lateral spreading on the wall target, the intensity of the initial jetting and the propagating shock waves in the air is reduced; however, the relative velocities between the penetrating water phase and the expelled surrounding gas remain significant.

In Figure 6, a characteristic time instance governed by a widespread spatial water dispersion is chosen to depict the functionality of the flow topology detection algorithm, along with the sub-grid scale information obtained under a diffuse interface approach. On the left side of the axis of symmetry are marked the previously sharply treated flow

regions, which satisfy both the geometric and topological criteria and thus, are subject to a diffuse interface formulation in the following time-step. As expected, these regions are detected on the borders of the already diffuse interface regions within the dispersed water cloud and they concern relatively large flow structures, which were previously resolvable by the mesh resolution with local minimum cell sizes of $10^{-5}$m. For the currently diffuse interface region within the highly dispersed droplet cloud, the calculated interface surface area density diameters are illustrated. As shown, the local diameters used for the local drag force calculation range from the spectrum of microscales to $10^{-5}$m, which is the local minimum cell size and correspondingly the limit for a sub-grid scale analysis.

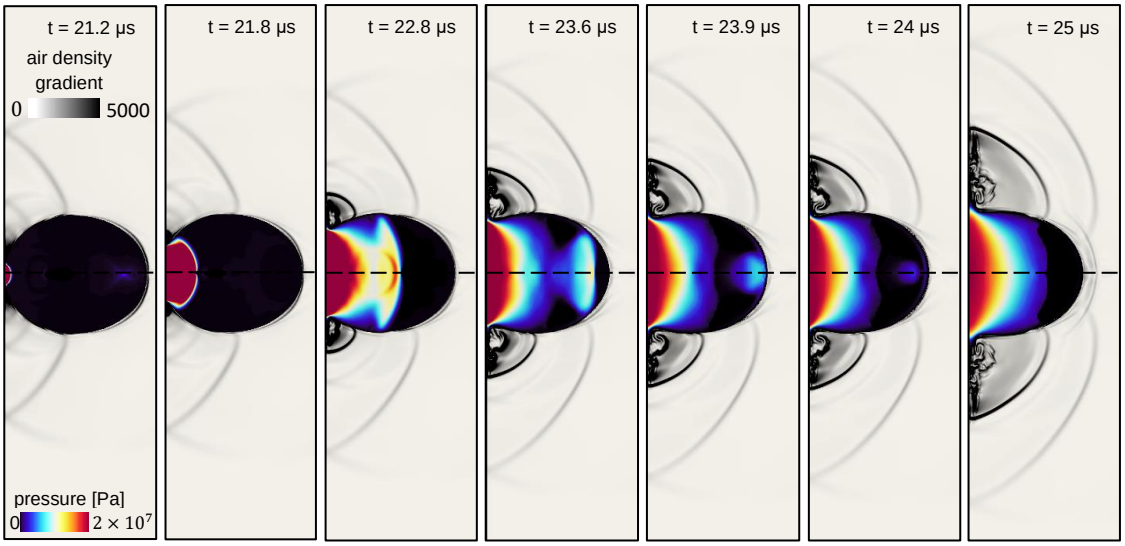


**Figure 5.** Time evolution of the pressure field inside the droplet, the strong shock wave formation and propagation, along with the density gradient and the propagating shock waves in the supersonic surrounding air after the droplet impact on the target.

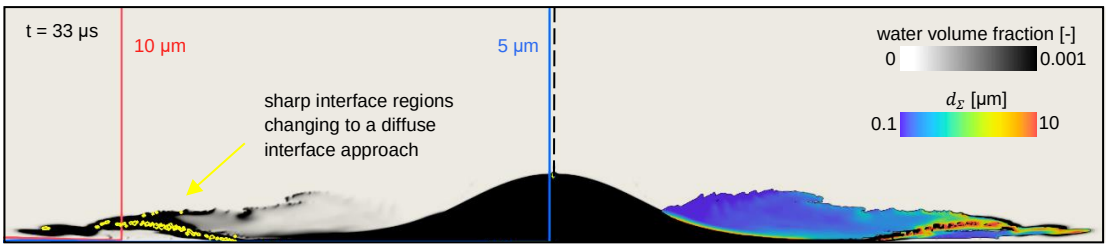


**Figure 6.** (on the left) In yellow are presented the sharp interface regions, which satisfy the topological criterion and will change to a diffuse interface approach, along with the limits in local computational grid resolution. (on the right) The dispersed flow region, which is subject to a diffuse interface approach and the calculated interface surface area density diameters.

## Conclusions

A compressible Σ-Y two-fluid model with dynamic interface sharpening based on local topological criteria has been developed and implemented in OpenFOAM® with the aim to simulate highly compressible flows with significant slip velocity effects and multiscale complexities. The overall model functionality has been thoroughly examined and applied in the highly compressible and multiscale case of a high-speed droplet impact; new experiments have been performed for a water droplet splashing onto a solid surface at Weber number ~$10^5$ that have not been previously reported in the literature. The obtained results have shown a good agreement with the conducted experimental study regarding the capturing of the macroscopic characteristics of droplet fragmentation. Additionally, the proposed model has provided significant advantages particularly under a dispersed flow regime which dominates the later stages of droplet splashing in comparison to numerical methods imposing a sharp interface. The developed multiscale two-fluid approach contributes with additional information regarding the physical phenomenon evolution, like the relative velocity field, the shock waves development and the interface surface area evolution, which have contributed to a better understanding and more accurate modelling of complex multiscale flow fields.

## Acknowledgements

The research leading to these results has received funding from the European Union's Horizon 2020 Research and Innovation programme under the Marie Skłodowska-Curie Grant Agreement No 675676.

## Nomenclature

| | |
|---|---|
| $\alpha$ | volume fraction [-] |
| $C_{SGS}$ | sub-grid scale mechanisms adjustable constant coefficient [-] |
| $d$ | diameter [m] |

$e$ specific internal energy [kJ/kg]
$g$ acceleration of gravity [m/s$^2$]
$k$ specific kinetic energy [kJ/kg]
$p$ pressure [Pa]
$\boldsymbol{q}^{eff}$ effective heat flux vector [W/m]
$\rho$ density [kg/m$^3$]
$\Sigma$ liquid gas interface surface area density [1/m]
$\Sigma^*$ equilibrium liquid gas interface surface area density [1/m]
$\boldsymbol{\tau}^{eff}$ effective stress tensor [Pa]
$\tau_{SGS}$ sub-grid scale mechanisms time scale [1/s]
$u$ velocity field [m/s]
$u_c$ artificial compression velocity field [m/s]
$u_m$ liquid and gaseous mixture velocity field [m/s]
$\psi$ compressibility [s/m]

**References**


[1] Dukowicz, J., 1980, “A Particle-Fluid Numerical Model for Liquid Sprays,” J. Comput. Phys., **35**, pp. 229–253.
[2] Drew, D. A., 1983, *Mathematical Modeling of Two-Phase Flow.*
[3] Ishii, M., and Mishima, K., 1984, “Two-Fluid Model and Hydrodynamic Constitutive Relations,” Nucl. Eng. Des., **82**(2–3), pp. 107–126.
[4] Vallet, A., Burluka, A. A., and Borghi, R., 2001, “Development of a Eulerian Model for the ‘Atomization’ of a Liquid Jet,” At. sprays, **11**(6).
[5] Lebas, R., Menard, T., Beau, P. A., Berlemont, A., and Demoulin, F. X., 2009, “Numerical Simulation of Primary Break-up and Atomization: DNS and Modelling Study,” Int. J. Multiph. Flow, **35**(3), pp. 247–260.
[6] Marchisio, D. L., Pikturna, J. T., Fox, R. O., Vigil, R. D., and Barresi, A. A., 2003, “Quadrature Method of Moments for Population-Balance Equations,” AIChE J., **49**(5), pp. 1266–1276.
[7] Navarro-Martinez, S., 2014, “Large Eddy Simulation of Spray Atomization with a Probability Density Function Method,” Int. J. Multiph. Flow, **63**, pp. 11–22.
[8] Vujanović, M., Petranović, Z., Edelbauer, W., Baleta, J., and Duić, N., 2015, “Numerical Modelling of Diesel Spray Using the Eulerian Multiphase Approach,” Energy Convers. Manag., **104**, pp. 160–169.
[9] Wardle, K., 2013, “Hybrid Multiphase CFD Simulation for Liquid-Liquid Interfacial Area Prediction in Annular Centrifugal Contactors,” *Global 2013*, pp. 1–9.
[10] Xu, L., Zhang, W. W., and Nagel, S. R., 2005, “Drop Splashing on a Dry Smooth Surface,” Phys. Rev. Lett., **94**(18), pp. 1–4.
[11] Thoroddsen, S. T., Takehara, K., and Etoh, T. G., 2012, “Micro-Splashing by Drop Impacts,” J. Fluid Mech., **706**, pp. 560–570.
[12] Guo, Y., Lian, Y., and Sussman, M., 2016, “Investigation of Drop Impact on Dry and Wet Surfaces with Consideration of Surrounding Air,” Phys. Fluids, **28**(7).
[13] Wu, Z., and Cao, Y., 2017, “Dynamics of Initial Drop Splashing on a Dry Smooth Surface,” pp. 1–11.
[14] Haller, K. K., Ventikos, Y., Poulikakos, D., and Monkewitz, P., 2002, “Computational Study of High-Speed Liquid Droplet Impact,” J. Appl. Phys., **92**(5), pp. 2821–2828.
[15] Niu, Y. Y., and Wang, H. W., 2016, “Simulations of the Shock Waves and Cavitation Bubbles during a Three-Dimensional High-Speed Droplet Impingement Based on a Two-Fluid Model,” Comput. Fluids, **134**–**135**, pp. 196–214.
[16] Kyriazis, N., Koukouvinis, P., and Gavaises, M., 2018, “Modelling Cavitation during Drop Impact on Solid Surfaces,” Adv. Colloid Interface Sci., **260**, pp. 46–64.
[17] Wu, W., Xiang, G., and Wang, B., 2018, “On High-Speed Impingement of Cylindrical Droplets upon Solid Wall Considering Cavitation Effects,” J. Fluid Mech., **857**, pp. 851–877.
[18] Nykteri, G., Koukouvinis, P., and Gavaises, M., “A Compressible Σ - Y Two -Fluid Atomization Model with Dynamic Interface Sharpening Based on Flow Topology Detection,” *ICLASS 2018, 14th International Conference on Liquid Atomization & Spray Systems*.
[19] Brackbill, J. U., Kothe, D. B., and Zemach, C., 1992, “A Continuum Method for Modeling Surface Tension,” J. Comput. Phys., **100**(335–354).
[20] Kelbaliyev, G. I., 2011, “Drag Coefficients of Variously Shaped Solid Particles , Drops , and Bubbles,” **45**(3), pp. 248–266.
[21] Lahey, R. T., 2005, “The Simulation of Multidimensional Multiphase Flows,” Nucl. Eng. Des., **235**(10–12), pp. 1043–1060.
[22] Ivings, M. J., Causon, D. M., and Toro, E. F., 1998, “On Riemann Solvers for Compressible Liquids,” Int. J. Numer. Methods Fluids, **28**(3), pp. 395–418.
[23] Deshpande, S. S., Anumolu, L., and Trujillo, M. F., 2012, “Evaluating the Performance of the Two-Phase Flow Solver InterFoam,” Comput. Sci. Discov., **5**(1).
[24] Andreini, A., Bianchini, C., Puggelli, S., and Demoulin, F. X., 2016, “Development of a Turbulent Liquid Flux Model for Eulerian-Eulerian Multiphase Flow Simulations,” Int. J. Multiph. Flow, **81**, pp. 88–103.
[25] Chesnel, J., Reveillon, J., Menard, T., and Demoulin, F. X., 2011, “Large Eddy Simulation of Liquid Jet Primary Breakup,” At. Sprays, **21**(9), pp. 711–736.
[26] Shonibare, O. Y., and Wardle, K. E., 2015, “Numerical Investigation of Vertical Plunging Jet Using a Hybrid Multifluid-VOF Multiphase CFD Solver,” Int. J. Chem. Eng., **2015**.